Axisymmetric Mixing Layer: Influence of the Initial and Boundary Conditions

Z. D. Husain* and A.K.M.F. Hussain†
University of Houston, Houston, Texas

The mixing layer in the near field of a 12.7-cm-diam circular air jet has been experimentally investigated at a jet speed of 30 m/s. Data have been obtained with a computer-traversed hot wire for laminar as well as equilibrium turbulent exit boundary layers, both without and with a large end plate. The integral measures of the mixing layer and their streamwise evolutions show essentially no dependence on the end plane geometry (i.e., exit boundary condition) except for a small x range ($x/\theta_e \simeq 500$) when initially laminar, but show strong dependence on the initial condition (i.e., laminar vs turbulent). The mean velocity and turbulence intensity profiles and streamwise spectral evolutions indicate that the shear layers have achieved self-preservation. Initially turbulent layers show two stages of linear growth; compared to the initially laminar layers, the growth rate is lower in the first stage but higher in the second stage. The turbulent field achieves self-similarity much later than the mean field when the initial state is turbulent, but essentially together when the initial state is laminar. The virtual origin is upstream of the lip for the initially laminar layers, but downstream for initially turbulent layers. Suprisingly, the present data are in both qualitative and quantitative agreement with plane mixing layer results. The Re_x range (up to 10^6) in this study is apparently insufficient to resolve the question of the asymptotic effect of the initial condition of a mixing layer.

Introduction

THE nonreacting, single-phase, isothermal, incompressible mixing layer of a Newtonian fluid is the simplest practical turbulent shear flow. Accumulated data reveal that even the simple integral measures of this reference flow have varied from experiment to experiment,[1-12] thus pointing to the inherent complexity of turbulent flows.

The mixing layer is a function of the initial condition (i.e., flow structure at the start of the layer), the boundary condition (i.e., the flow geometry), and the Reynolds number. Since the ratio of turbulent to molecular diffusivities (i.e., the Reynolds number) is large in a turbulent flow and since the Reynolds number in a mixing layer increases with x, the principle of Reynolds number similarity suggests that turbulent shear layers should achieve a universal state. The streamwise rate of evolution of the shear layer being slow, the principle of dynamic equilibrium suggests that the layer should progressively attain independence from the initial condition. Thus both the principles of asymptotic and local invariances suggest that all free mixing layers in the self-preserving region should be universal. In contrast, published data show considerable discrepancy, suggesting conflicting flow physics.

Our studies showing strong dependence of the near field of a plane jet on the exit plane flow characteristics suggested to us that the discrepancies in the shear layer data might be related to the initial condition.[1,3,6,12-14] Most early investigators did not document the initial condition, presumably on the assumption that the self-preserving state must be independent of it. (All future studies of near-field free shear flows should include documentation/calibration of the initial condition.) Our earlier measurements in a smaller (7.6-cm diam) nozzle showed that the mixing layer characteristics are independent of the initial momentum thickness but are strongly influenced by initial fluctuation characteristics.[10,11]

Received April 24, 1978; revision received Aug. 8, 1978.

Index categories: Jets, Wakes, and Viscid-Inviscid Flow Interactions; Hydrodynamics.

*Research Assistant.
†Professor. Member AIAA.

Parenthetically, continued pursuits of the mixing layer dynamics not only have failed to resolve these controversies, but have contributed to them as well. For example, Chandrasuda et al.[15] suggest that the vortex-roll-type Brown-Roshko structure is rare; it is merely a relic of upstream transition and the structure is indeed three-dimensional when the initial or the freestream turbulence is high. Oster et al.[16] found that a trip increased the spread rate of a one-stream mixing layer but decreased that of a two-stream mixing layer. In a subsequent study, Oster et al.[17] found no evidence of pairing when large entrainment was induced by controlled excitation. This observation contradicts convincing claims[2,4,18,19] that the pairing process is responsible for entrainment (i.e., entrapment).

Turbulent free shear flows appear to be dominated by large-scale coherent structures[2,4,16-18] whose initial formation through instability and rollup is determined by the initial condition. The structure resulting from each interaction like pairing depends on the structure preceding the pairing. As such, the initial condition may continue to retain control over a long distance. On the other hand, the structure at any x may be organized by feedback from downstream.[20,21]

It was decided to study the effect of two distinctly different initial boundary layers (viz., initially laminar and fully developed turbulent) and two distinctly different exit boundary conditions (i.e., no exit plate and a large exit plate). Since effects of these changes are expected to be felt for a limited length from the lip, the ease of modification of these conditions suggested the choice of the axisymmetric mixing layer. In order to make a large change in the exit plane geometry, an end plate of a diameter about 12 times the jet diameter was considered adequate.

Apparatus and Procedure

Data were taken in a 12.7-cm-diam air jet. Air from a filter box (removes 95% of 0.5-μ diam particles) enters the six-blade centrifugal blower driven by a dc motor. Air from the blower moves through a 1.0-m-long muffler box designed to suppress high-frequency acoustic components. Following the muffler box is a 1.3-m-long straightener box of rectangular cross section (33 cm × 26 cm). The flow then passes through a 12-deg square diffuser, fitted with four screens, and finally through ten screens before exiting through an axisymmetric

nozzle (36:1 contraction ratio). The nozzle is 76 cm long and has a contour which is a compromise between the Batchelor-Shaw and the cubic equation shapes.[22] The nozzle is terminated with a metal ring to which nozzle tips of various lengths and various trip rings can be attached. A 6.35-cm-long tip with a wedge angle of 20 deg is used for the initially laminar cases (Fig. 1a). Various trip rings along with the 6.35-cm-long tip showed that the boundary layer, though tripped, was not developed and that the spectral broadening was incomplete at the lip. Subsequently, a 25-cm-long tip was used to obtain a fully developed turbulent boundary layer at the exit. A 1-cm-thick aluminum ring projecting 0.08 cm inside the nozzle wall (with its inner face knurled for inducing three-dimensional disturbances) was used to trip the boundary layer before the tip (Fig. 1b). In order to study the effect of the end plane geometry (i.e., the boundary condition), a 1.50-m-diam exit plate was so attached that the jet exits normal to and through its center (Fig. 1c); care was taken to fill and smooth the surfaces. The exit plate diameter, being an order of magnitude larger than the jet diameter, was considered adequate for demonstrating the exit boundary-condition effect. Because of the falloff of the entrainment velocity as the inverse of the radius, a rounded leading edge at the rim of the exit plate was considered unnecessary. The coordinate system of the flow is shown in Fig. 1d.

The jet discharges into a large laboratory (30 m × 15 m × 3.5 m) with controlled temperature, humidity, and traffic. The hot-wire traverse, with a resolution of 0.0254 mm, is performed by a four-coordinate (x,y,z,ϕ) automated traversing mechanism (backlash free) operated by stepping motors under software control from the on-line laboratory computer (HP 2100S) located in an adjoining room. Analog data are transmitted to the computer through a 25-m-long cable provided with termination networks so that the signal is free from distortion/reflection up to 100 kHz. Data were digitized with the help of a 12-bit A/D converter (204 kHz), built in-house. Data were obtained with a 2-mm-long 4-μ-diam tungsten hot wire operated at an overheat ratio of 1.4 with linearized TSI 1050 series anemometers. The spectra data were obtained with a Spectrascope SD335 (500 lines) real-time spectrum analyzer. Each spectrum plot presented is an ensemble average of 128 separate realizations.

The initial boundary layer was characterized as turbulent when four different criteria were satisfied simultaneously: the shape factor should be close to 1.4; the mean velocity profile should show clear logarithmic and wake regions in (U^+, Y^+) coordinates; the longitudinal one-dimensional frequency spectrum should be continuous and broadband; and the turbulence intensity profile $u'(y)$ should monotonically increase as the wall is approached, reaching a maximum essentially at the wall, i.e., at $y \lesssim 0.1\delta_I$; δ_I is the boundary-layer displacement thickness defined as $\int_0^\infty (1-U/U_e)\,dy$. Even in a jet with an initially laminar boundary layer, there will be significant u' within the boundary layer, its profile having the peak value noticeably away from the wall, typically at $y \simeq \delta_I$, and the spectra characterized by low, discrete frequencies. These fluctuations can be attributed to cavity resonance frequencies[12] and blower blade passage frequency, which are responsible for most of the exit centerline fluctuation intensity. Acoustic suppression tests were done with Helmholtz resonators and quarter-wave tubes attached to the straightener box but improvements were marginal, presumably because the settling chamber resonant modes are too strong to be suppressed by the reactive resonators.

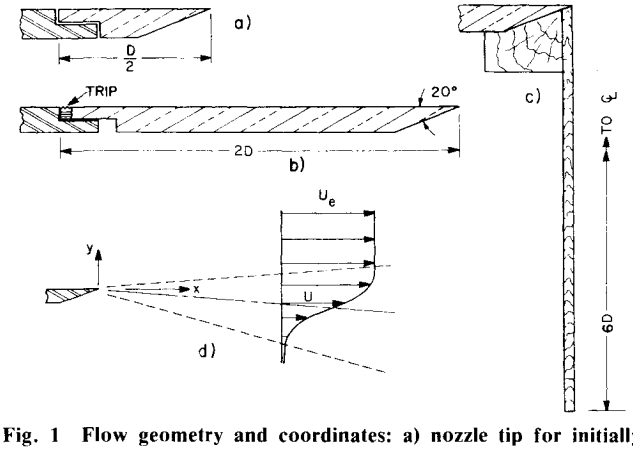

Fig. 1 Flow geometry and coordinates: a) nozzle tip for initially laminar boundary layers; b) nozzle tip for initially fully developed turbulent boundary layers; c) end plate geometry for both initial conditions; d) flow coordinates.

Table 1 Initial integral parameters

		δ_I, cm	θ, cm	δ_I/θ	$U_e\theta/\nu$
Laminar:	without end plate	0.0536	0.0211	2.533	432
	with end plate	0.0538	0.0216	2.503	442
Turbulent:	without end plate	0.1011	0.0706	1.432	1445
	with end plate	0.0917	0.0632	1.453	1294

Results and Discussion

For all the data presented here, the characteristic velocity U_e was 30 m/s and the freestream turbulence intensity, 0.34%. The exit plane mean velocity and fluctuation intensity profiles, measured at 1 mm downstream from the lip, are shown in Fig. 2a for the initially laminar cases and in Fig. 2b for the initially turbulent cases. The corresponding initial integral parameters are given in Table 1.

Even though the addition of the end plate drastically changes the exit boundary condition, the changes in the initial integral measures, viz. δ_I and θ, are marginal; the shape factor is essentially unchanged. The mean profiles for the initially laminar cases agree well with the Blasius profile (Fig. 2a). Most of the disturbances in the initially laminar case occurred at discrete frequencies predominantly below 150 Hz; these frequencies can be attributed to the jet settling chamber cavity resonance modes and blade passage and are about an order of magnitude lower than the instability frequency of the shear layer (discussed later). The only noticeable effect of the addition of the exit plate is on the exit fluctuation intensity profile (at 1 mm downstream from the lip), presumably due to the interaction of the transverse boundary layer on the end plate and the free shear layer. However, the true initial condition must be taken upstream of the lip where the flow structure should be the same with and without the end plate.

To what extent does the initial boundary layer in the turbulent case compare with the equilibrium flat plate turbulent boundary layer? Most previous investigators failed to adequately address this important question.[10,11,14] The tripped boundary layers in the experiments of Brown and Roshko,[2] Champagne et al.,[3] and Batt[6] probably failed to produce intially turbulent boundary layers.[15] Figure 2c shows the initial mean velocity distribution in the universal coordinates (U^+, Y^+) for the turbulent case without the end plate. The friction velocity $U_*(\equiv\sqrt{T_w/\rho}) = U/U^+$ was determined by the cross plot (Clauser plot) technique[23] and was found to be 0.0453 U_e. The data clearly show a significant extent of the logarithmic region, which is compared with the universal relation $U^+ = 5.6 \log_{10} Y^+ + 4.9$. The wake region of the profile is typical of flat plate boundary layers; the wake strength $\Delta U^+ = 1.5$ for $U_e\theta_e/\nu \simeq 1400$ agrees with that expected for flat plate equilibrium boundary layers.[24] The shape factor ($\simeq 1.44$) is close to the flat plate value. Figure 2b shows comparison of our u'/U_e data with those of Klebanoff replotted from Ref. 25 by assuming $\delta/\delta_I = 7$. (Most publications report only δ, whose determination from data is not unambiguous; more deterministic length scales like δ_I or θ

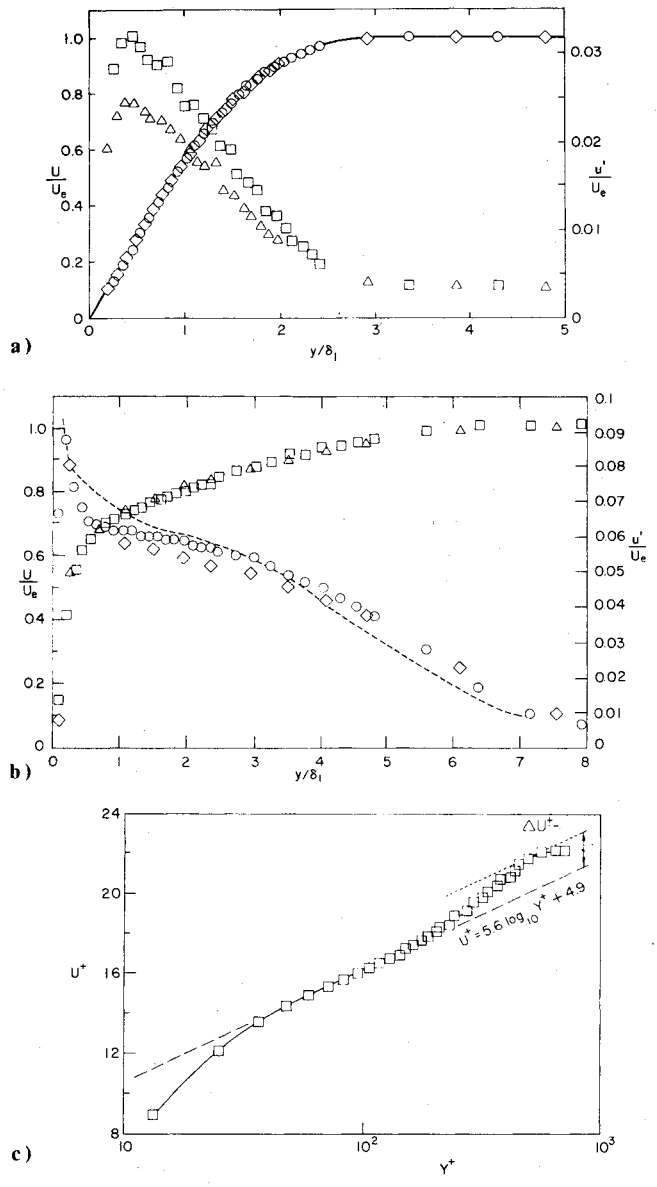

Fig. 2 a) Initial mean velocity and longitudinal intensity profiles for the initially laminar cases. Without end plate: ○, U/U_e; △, u'/U_e. With end plate: ◇, U/U_e; □, u'/U_e. ——, Blasius profile. b) Initial mean velocity and longitudinal turbulence intensity profiles for the initially turbulent cases. Without end plate: □, U/U_e; ○, u'/U_e. With end plate: △, U/U_e; ◇, u'/U_e ---, Klebanoff's flat plate data ($U_*/U_e = 0.037$, $U_e\delta/\nu = 8\times10^4$). c) Initial mean velocity distribution for the case with the same symbols as in Fig. 2b; $U^*/U_e = 0.0453$; ΔU^+: wake strength.

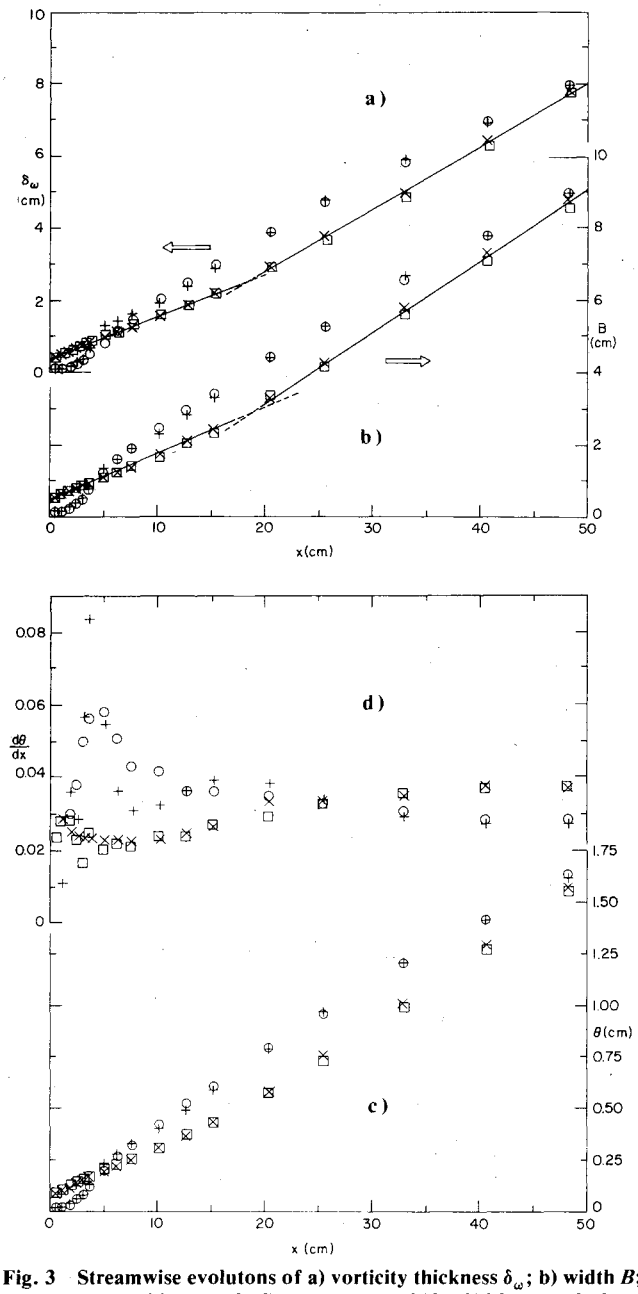

Fig. 3 Streamwise evolutons of a) vorticity thickness δ_ω; b) width B; c) momentum thickness θ; d) spread rate $d\theta/dx$. Without end plate: ○, laminar; □, turbulent. With end plate: +, laminar, ×, turbulent.

should be reported so that data from different experiments can be compared.) The small discrepancies between our data and Klebanoff's are understandable: at low y/δ_l the discrepancy is due to the fact that the measurements are in the free shear layer (at 1 mm downstream from the lip) and the discrepancy at large y/δ_l is due to the fact that the centerline turbulence intensity in our jet is higher than that in Klebanoff's closed-loop tunnel. The u-spectrum anywhere in the initial boundary layer is monotonic and broadband up to 10 kHz (see Fig. 5c). Thus the initially turbulent cases compare well with the equilibrium flat plate turbulent boundary layer.

The shear layer thickness is a measure of momentum exchange and can be represented by the width $B \equiv (y_{0.95} - y_{0.10})$, the momentum thickness $\theta \equiv \int_{-\infty}^{\infty} (U/U_e)(1 - U/U_e)\,dy$, or the vorticity thickness $\delta_w \equiv U_e/(\partial U/\partial y)_{max} = (1/|\omega|_{max}) \int_{-\infty}^{\infty} |\omega|\,dy$; $y_{0.95}$ and $y_{0.1}$ are the y locations where U/U_e is 0.95 and 0.1, respectively. Figures 3a, b, and c show the streamwise evolutions of $\delta_w(x)$, $B(x)$, and $\theta(x)$, respectively. In order to eliminate the error on the low-velocity side due to large velocity fluctuations and the transverse entrainment velocity, profile integration is terminated at $y = y_{0.1}$ in the calculation of θ. Being an integral quantity, θ is not sensitive to the details of the profile. δ_w is a more desirable measure of the shear layer width, since it is independent of the low-speed side measurement; it was determined from the slope of the least-square-fit error function through the data between $y_{0.95}$ and $y_{0.1}$. Except for the self-preserving region, where θ, B, and δ_w should be uniquely related, Figs. 3a, b, and c provide somewhat independent information since δ_w is weighted by the middle of, B by the edges of, and θ by the entire, mixing layer.

The B, θ, and δ_w data manifest somewhat similar trends. First, the stramwise variations of these quantities are independent of whether there is an exit plate or not. These thicknesses for the initially laminar cases grow rapidly up to about $x = 5$ cm; then the rate of growth progressively decreases. The streamwise variations are not linear, even

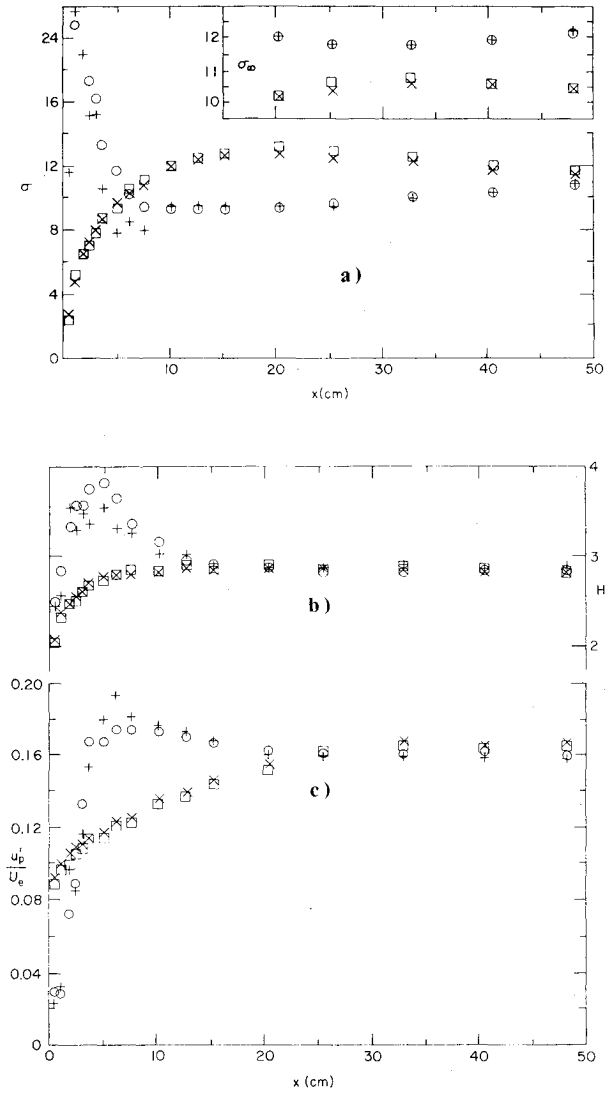

Fig. 4 a) Streamwise evolutions of σ and σ_∞; b) Streamwise evolutions of the shape factor; c) Streamwise evolutions of u_p'/U_e. For legend see Fig. 3a.

though data for $x \geq 20$ cm can be approximated by a straight line. These thicknesses for the initially turbulent cases, even though always larger than those for the initially laminar cases at the exit plane, grow initially slowly and then rapidly, but do not exceed the initially laminar values even at the end of the x range of this experiment (Figs. 3a, b, and c). For the initially turbulent cases, the streamwise variations of B or θ can be closely fitted with two straight lines.[10] The slope of the second line is noticeably higher than that of the first line, and the changeover occurs at about $x = 20$ cm ($\simeq 300\ \theta_e$). The changeover remains unexplained, but may be related to the change in the coherent structure from that in the initial thin shear layer to the axisymmetric jet structure, and is the focus of a new investigation in our laboratory. Only Foss[14] and Browand[29] have found such slope changes, but both in plane layers. We take the second stage as the self-preserving region and accordingly define the virtual origin x_0. Figures 3a, b, and c show that the virtual origin is upstream of the lip for initially laminar cases but downstream for the turbulent cases. Our data contrast the conclusion of Champagne et al.[3] that the virtual origin is predominantly downstream of the lip for initially laminar cases but agrees with Brown and Roshko's[2] observations. Bradshaw[1] found that $x_0 \simeq 150\ \theta_e$ for initially turbulent layers and $-200 < x/\theta_e < 350$ for laminar cases. However, other studies[6,9,14] found the virtual origin upstream of the lip for initially tripped boundary layers.

The spread rates $d\theta/dx$ and dB/dx in the self-preserving region is higher for the turbulent cases compared to those in the laminar cases, suggesting that entrainment in the former cases are higher. However, values of the spread rates are higher for the laminar cases in the region 2.5 cm $\lesssim x \lesssim$ 20 cm. At least for the plane mixing layer, $d\theta/dx$ can be shown to be V_E/U_e where V_E is the entrainment velocity, typically around 3% of U_e. Values of $d\theta/dx$, shown in Fig. 3d, were determined by passing a least-square-fit cubic equation through five adjacent data points and taking its slope at the midpoint. The large value of $d\theta/dx$ at $x \simeq 5$ cm, for the laminar cases, may be associated with the first pairing of the mixing layer rolled-up vortex in the "shear layer mode."[18] This interpretation is consistent with the notion that most of the mixing layer entrainment is due to large-scale coherent structure interactions.[4,16-19] The disagreement between the two laminar cases at $x \approx 7$ cm indicates influence of the end plate, probably through influencing the first pairing of the rolled-up vortices. For the initially turbulent cases, the noticeable change in $d\theta/dx$ at $x \simeq 20$ cm may also be associated with the organized structure interaction like pairing, presumably occurring in the "jet mode."[18] The fine-grained turbulence of the tripped shear layer acts to lower the effective Reynolds number so that this layer also can undergo large-scale instability, rollup due to nonlinear saturation, and then pairup. This conjecture will be tested in the laboratory through careful investigation in the mixing layer of a larger (18-cm diam) axisymmetric jet and in a 91-cm-span plane mixing layer.

The streamwise variations of the similarity parameter σ corresponding to the Tollmien profile[26] are shown in Fig. 4a and the profile shape factor $H = \delta_1/\theta$ is shown in Fig. 4b. These show the inherent differences between the evolutions of initially laminar and turbulent layers; σ shows the effect on the details of the profile and H the integral effect. Data in these two figures clearly show that the profile shapes are unaffected by the exit plate.

Even though σ is meaningful only in the self-preserving region, it is a measure of the variation of the profile shape. For initially laminar cases, σ increases rapidly, then decreases rapidly until $x \simeq 5$ cm before gradually increasing again. For initially turbulent layers, σ increases monotonically until $x \simeq 20$ cm before decreasing gradually farther downstream. If the virtual origin is taken into account, the values of σ attain essentially constant values σ_∞ in the self-preserving region 20 cm $\lesssim x \lesssim$ 50 cm (see insert in the right-hand top corner in Fig. 4a); average values of σ_∞ are 11.94 for the laminar cases and 10.47 for the turbulent cases. If the profile is represented by an error function, $d\delta_w/dx = \sqrt{\pi}/\sigma$; thus σ is a measure of the spread rate. The largest differences due to the end plate, even though by no means significant, appear to be at $x \simeq 5$ cm for the laminar cases and $x \simeq 20$ cm for the turbulent cases. These were identified as the possible locations for maximum coherent structure activity like pairing.

The evolution of the shape factor H is dependent on the initial condition for $x \lesssim 15$ cm, after which it reaches the constant value of 2.845.

The streamwise evolutions of the peak fluctuation intensity u_p'/U_e are shown in Fig. 4c for the four initial conditions. For the initially laminar cases, the peak intensity increases exponentially due to linear instability, reaches its maximum due to nonlinear saturation at $x \simeq 6$ cm before progressively decreasing downstream. For the initially turbulent cases, u_p'/U_e increases monotonically due to growth-retarding nonlinear effects of the already-present broadband turbulence, but slightly exceeds the laminar value at $x \geq 25$ cm. The evolutions of H and u_p'/U_e are somewhat similar. Except for the peak values for the initially laminar cases, the fluctuation intensity data are, within the experimental uncertainty, independent of the presence of the exit plate. Note that the asymptotic values of u_p'/U_e are 0.159 and 0.166 for the laminar and turbulent cases, respectively. Batt[6] found

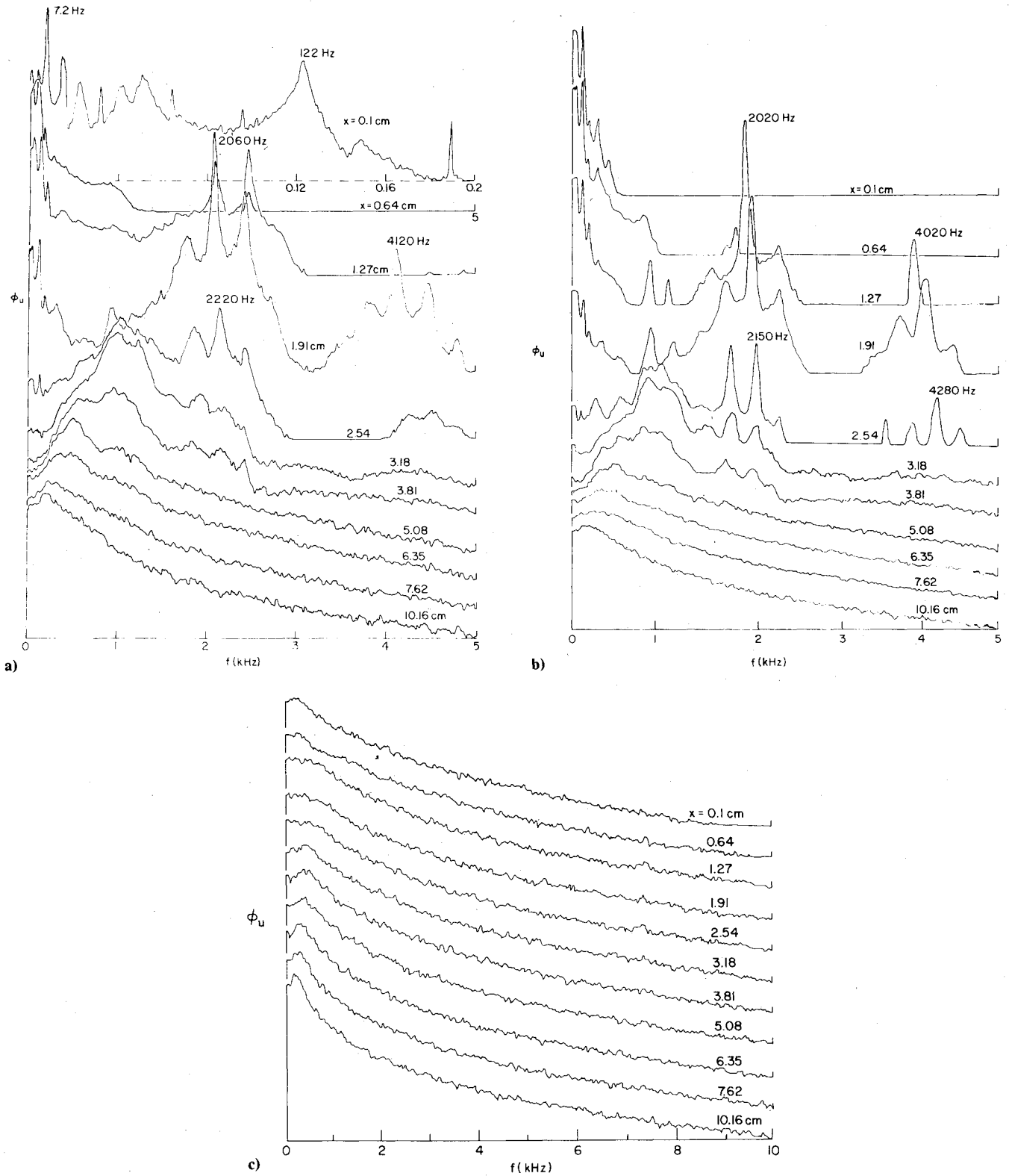

Fig. 5 Evolutions of ϕ_u along $U/U_e = 0.8$ for initially laminar boundary layer: a) without end plate; b) with end plate; c) evolutions of ϕ_u along $U/U_e = 0.8$ for initially turbulent cases.

these values to be 0.16 and 0.17, respectively. The asymptotic values reported in the literature are 0.12,[4] 0.147,[8] 0.17,[3,14] 0.176,[7,9] and 0.19.[5]

Further investigation of the evolution of the free shear layer was attempted by measuring the longitudinal one-dimensional frequency spectrum ϕ_u. In order to capture the large-scale activity in the mixing layer, it was decided to measure ϕ_u at the y location where $U/U_e = 0.8$. From our study as well as others,[27] this location appears to be the optimum choice. Figures 5a-c show the streamwise evolutions of ϕ_u for the initial conditions; since the spectral evolutions for the two initially turbulent cases are almost identical, only one (Fig. 5c) is presented; these are log-linear plots with arbitrary vertical scales. ϕ_u is defined such that $\int_0^\infty \phi_u^2(f)\,df = \overline{u^2}$. While the spectral evolutions are different for the four cases, it is clear that the broadening is complete by $x \simeq 10$ cm, indicating full development of each of the mixing layers.

For the initially laminar cases, the streamwise evolutions of ϕ_u contain interesting details of the flow physics. For discussion, let us limit ourselves to one case only, say Fig. 5b.

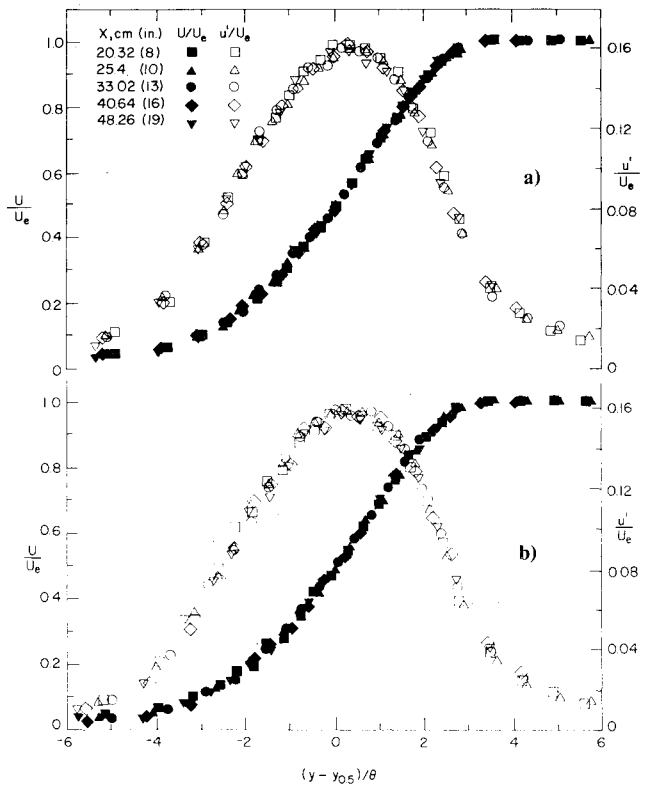

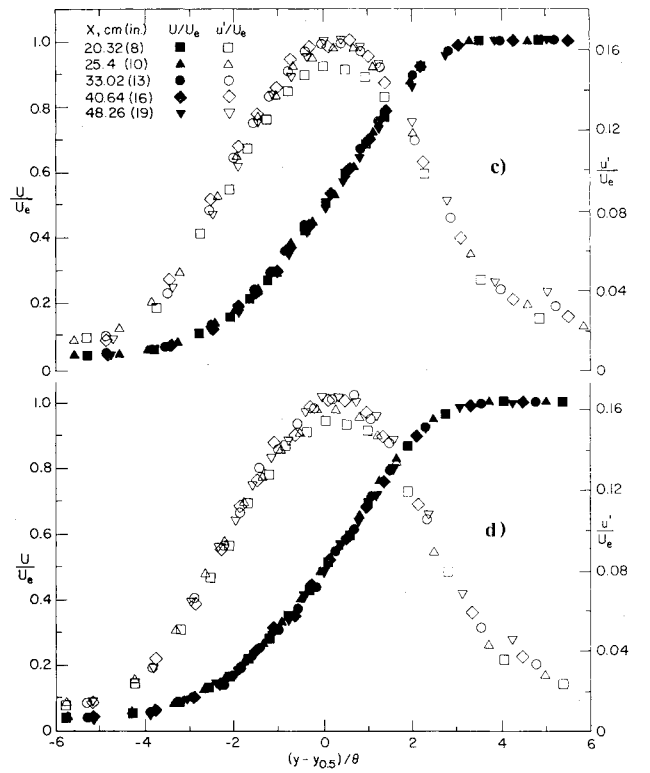

Fig. 6 Profiles of U/U_e and u'/U_e in the self-preserving region: a) initially laminar cases without end plate; b) initially laminar case with end plate; c) initially turbulent case without end plate; d) initially turbulent case with end plate.

The large peak at $x=1.27$ cm is the shear layer instability frequency (2020 Hz). Note that the initial condition spectral peaks, due to tunnel acoustic modes and blower blade passage, are at frequencies (essentially all below 150 Hz) too low to affect the shear layer dynamics and growth.[17] The variations in the apparent instability frequency with x are real, being due to the hot wire probe-induced shear tone effect.[21] The large number of peaks say at $x=2.54$ cm, is due to vortex pairing in the "shear layer mode."[18] It is interesting to note that the subharmonic peak frequency progressively decreases with increasing x, presumably due to (random) occurrence of subsequent pairing.

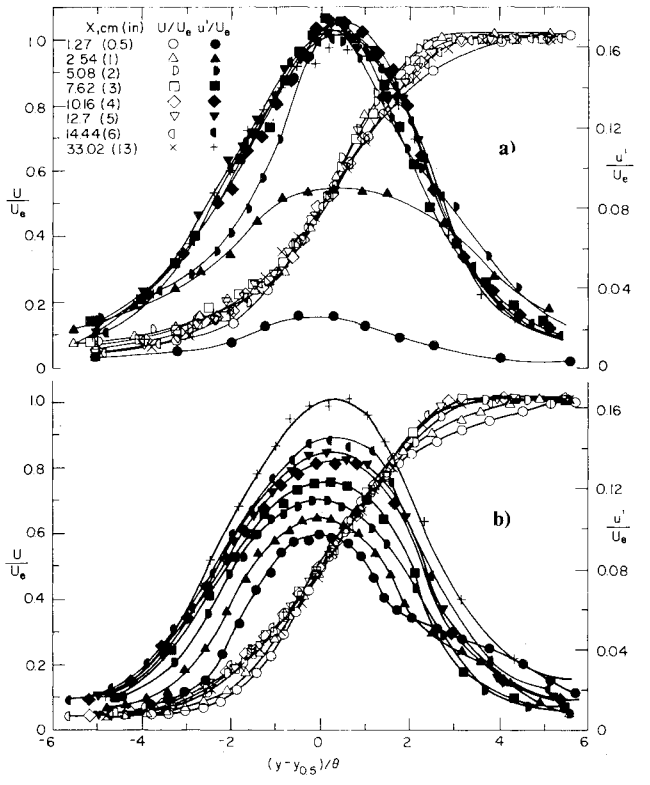

Fig. 7 Streamwise evolutions of U/U_e and u'/U_e profiles without end plate: a) initially laminar; b) initially turbulent.

For the turbulent cases, the initial spectra are monotonic functions of frequency, with spectral contents up to 10 kHz. These data confirm that both the turbulent cases originate from fully developed turbulent boundary layers. Note that the initial condition effect is "spectrally lost" at $x \gtrsim 7$ cm (Figs. 5a-c).

The question naturally arises as to whether the flows have achieved self-preservation, especially because of the limited streamwise extent of any axisymmetric mixing layer. In order to answer this question, the appropriate length scale to be used should be the distance from the virtual origin. However, in view of some uncertainty involved in the graphical determination of the virtual origin, it was decided that the meaningful length scale is an appropriately defined local length scale, say θ. Since sufficiently far away from the virtual origin, the flow can only be a function of $x-x_0$, it is clear that B, θ, and δ_ω should all be proportional to $x-x_0$. Consequently, choice of θ as the length scale is equivalent to a linear stretching of the usual transverse coordinate $(y-y_{0.5})/(x-x_0)$.

The profiles of mean velocity and turbulent intensity for the four cases are shown in Figs. 6a-d and confirm, within the experimental uncertainty, the achievement of (apparent) self-preservation of the free shear layer. In order to determine how rapidly the mean profiles achieve self-similarity compared to the turbulence intensity profiles, the streamwise evolutions are shown for two cases: Fig. 7a for the laminar case and Fig. 7b for the turbulent case, both without the end plate. While the evolution rates for the mean profiles are not noticeably different for laminar and turbulent cases, those of the fluctuation profiles are. The fluctuation intensity profiles achieve self-similarity much earlier in x for the laminar case than the turbulent case. For the laminar initial cases, turbulence profiles achieve essential self-similarity at $x \simeq 18$ cm

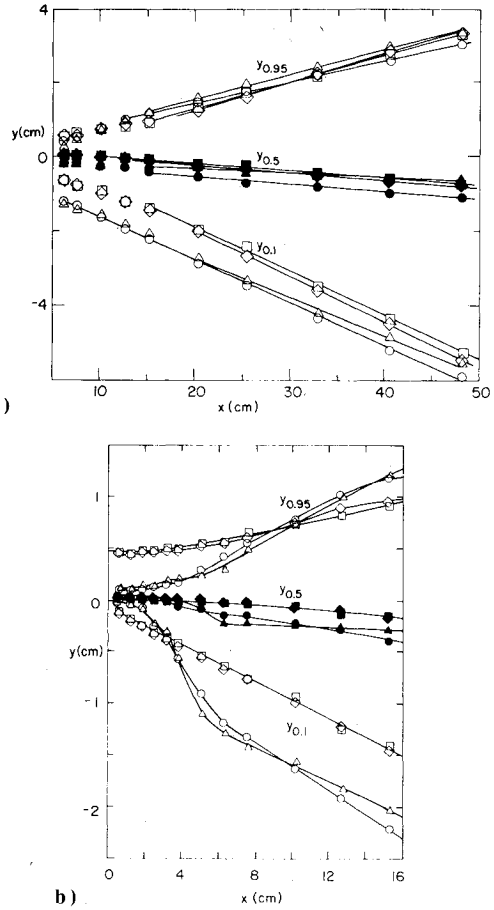

Fig. 8 Boundaries of the mixing layers for the x range: a) 5-50 cm; b) 0-16 cm. Without end plate: ○, laminar; □, turbulent. With end plate: △, laminar; ◇, turbulent. Solid symbols represent $y_{0.5}$.

($\simeq 850\theta_e$). For the initially turbulent case, the intensity profiles achieve self-similarity by 30 cm ($\simeq 450\theta_e$). The latter distance is considerably lower than the value of $1000\theta_e$ suggested by Bradshaw[1] or $1500\theta_e$ by Batt,[6] but agrees with the observations of Brown and Roshko.[2] Figures 6 and 7 also confirm our eariler observation that for initially turbulent layers, the mean field self-preservation significantly precedes that of turbulence field while both fields achieve self-similarity essentially together when initially laminar.

Figure 8a shows the boundaries in the self-preserving region and Fig. 8b, in the initial region. Note the inherent differences in the initiations of initially laminar and turbulent shear layers; the roll-up process for the initially laminar cases is evident (Fig. 8b). Even though the widths are somewhat different, the average boundaries in the self-preserving region are indeed linear (Fig. 8a).

Concluding Remarks

The discrepancies among published shear layer data, presumed to be due to effects of different initial and boundary conditions existing in different experiments, were explored by measuring the average characteristics of four mixing layers: two asymptotically limiting initial conditions, viz., laminar vs turbulent, each with two distinctly different boundary conditions, viz., with and without a large diameter end plate.

The results show that the two boundary conditions produce essentially identical evolutions for the mixing layer, for either choice of the initial condition, demonstrating that the presence or extent of the exit plate is irrelevant to the mixing layer average measures in the (apparent) self-preserving region. For the initially laminar cases, there is a noticeable effect of the exit plane geometry (i.e., boundary condition) for a small x range ($x/\theta_e \simeq 500$), presumably through modification of the initial vortex rollup and pairing. Batt[6] noted that the plane shear layer behaviors with and without an end plate were nearly identical but neither showed any data nor discussed the extent of this effect. The evolution of the mixing layer depends significantly on the initial state: laminar or turbulent. The differences between these two initial states have been discussed.

It is interesting to note that the linear variations of the widths and the constant asymptotes of H, σ_∞, $d\theta/dx$, $u'_{p\infty}$ continue unaffected through the last data station, at the end of the potential core, where the coherent structure undergoes a large change. In spite of the inherent differences between plane and axisymmetric shear layers,[28] there is an amazing extent of both qualitative and quantitative agreement of the present data with the plane shear layer data of Foss[14] and Batt,[6] especially on δ_ω, $u'_{p\infty}$, spread rate, etc. The location $x/\theta_e \simeq 300$ for spread rate change in the turbulent initial case coincides with Foss's data. Browand[29] and Birch[30] suggest that the spread rate in the second stage of the turbulent case is identical with the laminar case spread rate. Foss's[14] and the present data show different spread rates for the two cases.

We have not presented here any new findings of the coherent structures, which probably control the shear layer measure. It is not clear, however, that even detailed knowledge of the coherent structures will one day explain away the discrepancies in the published data. Since most discrepancies center around average measures, which are of technological importance, the data presented are significant on their own and may serve as references for the development/calibration of turbulent shear flow codes/theories.

Choice of the larger size of the nozzle still did not resolve the question of whether initially laminar and turbulent free shear layers evolve to identical asymptotic states. While both the principles of local and asymptotic invariances suggest such a state, it is not likely that such a state can be achieved in a practical, axisymmeteric mixing layer. It appears that equilibrium of the mixing layer, especially of its large-scale coherent structure, must be relegated to a state essentially an infinite distance away from the origin. The speculations by a number of investigators[14,30-32] must be tested in a long (as well as wide) plane mixing layer; such a layer is being investigated in our laboratory.

Acknowledgment

The authors are grateful to S. J. Kleis, J. F. Foss, and R. G. Batt for careful reviews of the manuscript and to the National Science Foundation and the Office of Naval Research for financial support.

References

[1] Bradshaw, P., "Effects of Initial Conditions on the Development of a Free Shear Layer," *Journal of Fluid Mechanics*, Vol. 26, 1966, pp. 225-236.

[2] Brown, G. L. and Roshko, A., "On Density Effects and Large Structures in Turbulent Mixing Layers," *Journal of Fluid Mechanics*, Vol. 64, 1974, pp. 775-816.

[3] Champagne, F. H., Pao, Y. H., and Wygnanski, I., "On the Two-Dimensional Mixing Region," *Journal of Fluid Mechanics*, Vol. 74, 1976, pp. 209-250.

[4] Winant, C. D. and Browand, F. K., "Vortex Pairing: The Mechanism of Turbulent Mixing-Layer Growth at Moderate Reynolds Number," *Journal of Fluid Mechanics*, Vol. 63, 1974, pp. 237-255.

[5] Spencer, B. W. and Jones, B. G., "Statistical Investigation of Pressure and Velocity Field in the Turbulent Two-Stream Mixing Layer," AIAA Paper 71-613, Palo Alto, Calif., 1971.

[6] Batt, R. G., "Some Measurements on the Effect of Tripping the Two-Dimensional Shear Layer," *AIAA Journal*, Vol. 13, Feb. 1975, pp. 245-247.

[7] Patel, R. P., "An Experimental Study of a Plane Mixing Layer," *AIAA Journal*, Vol. 11, Jan. 1973, pp. 67-71.

[8] Liepmann, H. W. and Laufer, J., "Investigation of Free Turbulent Mixing," NACA TN-1257, 1947.

[9] Wygnanski, I. and Fiedler, H. E., "The Two-Dimensional Mixing Region," *Journal of Fluid Mechanics*, Vol. 41, 1970, pp. 327-361.

[10]Hussain, A.K.M.F. and Zedan, M. F., "Effects of the Initial Condition on the Axisymmetric Free Shear Layer: Effects of the Initial Momentum Thickness," *The Physics of Fluids*, Vol. 21, 1978, pp. 1100-1112.

[11]Hussain, A.K.M.F. and Zedan, M. F., "Effects of the Initial Condition on the Axisymmetric Free Shear Layer: Effect of the Initial Fluctuation Level," *The Physics of Fluids*, Vol. 21, Sept. 1978, pp. 1475-1481.

[12]Hussain, A.K.M.F. and Clark, A. R., "Upstream Influence on the Near-Field of a Plane Turbulent Jet," *Physics of Fluids*, Vol. 20, 1977, pp. 1416-1426.

[13]Hussain, A.K.M.F. and Thompson, C.A, "Organized Motions in a Plane Turbulent Jet Under Controlled Excitation," *Proceedings of the 12th Annual Meeting, Society of Engineering Science*, University of Texas, Austin, Tex., 1975, pp. 741-752.

[14]Foss, J. F., "The Effects of the Laminar/Turbulent Boundary Layer States on the Development of a Plane Mixing Layer," *Symposium on Turbulent Shear Flows*, The Penn State University, University Park, Pa., April 1977, pp. 11.33-11.42.

[15]Chandrasuda, C., Mehta, R. D., Weir, A. D., and Bradshaw, P., "Effect of Free-Stream Turbulence on Large Structure in Turbulent Mixing Layers," *Journal of Fluid Mechanics*, Vol. 85, 1978, pp. 693-704.

[16]Oster, D., Wygnanski, I., and Fiedler, H., "Some Preliminary Observations on the Effect of Initial Conditions on the Structure of the Two-Dimensional Turbulent Mixing Layer," private communication, 1977.

[17]Oster, D., Dziomba, B., Fiedler, H., and Wygnanski, I., "On the Effect of Initial Conditions on the Two Dimensional Turbulent Mixing Layer," *Structure and Mechanisms of Turbulence I*, edited by H. Fiedler, Springer, New York, 1978, pp. 48-64.

[18]Hussain, A.K.M.F. and Zaman, K.B.M.Q., "Controlled Perturbation of Circular Jets," *Structure and Mechanisms of Turbulence I*, edited by H. Fiedler, Springer, New York, 1978, pp. 31-42.

[19]Hussain, A.K.M.F. and Zaman, K.B.M.Q., "Effect of Acoustic Excitation on the Turbulent Structure of a Circular Jet," *Proceedings of the Third Interagency Symposium on University Research in Transportation Noise*, University of Utah, Salt Lake City, Utah, 1975, pp. 314-325.

[20]Dimotakis, P. E. and Brown, G. L., "Large Structure Dynamics and Entrainment in the Mixing Layer at High Reynolds Numbers," *Journal of Fluid Mechanics*, Vol. 78, 1976, pp. 535-560.

[21]Hussain, A.K.M.F. and Zaman, K.B.M.Q., "The Free Shear Layer Tone Phenomenon and Probe Interference," *Journal of Fluid Mechanics*, Vol. 87, 1978, pp. 349-384.

[22]Hussain, A.K.M.F. and Ramjee, V., "Effects of the Axisymmetric Contraction Shape on Incompressible Turbulent Flow," *Journal of Fluids Engineering*, Vol. 98, 1976, pp. 58-69.

[23]Kline, S. J., Reynolds, W. C., Schraub, F. A., and Runstadler, P. W., "The Structure of Turbulent Boundary Layers," *Journal of Fluid Mechanics*, Vol. 30, 1967, pp. 741-773.

[24]Coles, D. E., "The Turbulent Boundary Layer in a Compressible Fluid," The Rand Corporation, Rept. R-403-PR, Sept. 1962.

[25]Zilberman, M., Wygnanski, I., and Kaplan, R. E., "Transitional Boundary Layer Spot in a Fully Turbulent Environment," *The Physics of Fluids*, Vol. 20, 1977, pp. S258-S271.

[26]Abramovich, N., *The Theory of Turbulent Jets*, M.I.T. Press, Cambridge, Mass., 1963.

[27]Lau, J. C. and Fisher, M. J., "The Vortex-Street Structure of 'Turbulent Jets,' Part 1," *Journal of Fluid Mechanics*, Vol. 67, 1975, pp. 299-337.

[28]Laufer, J., private communication, 1978.

[29]Browand, F. K., private communication, 1978.

[30]Birch, S. R., private communication, 1977.

[31]Fiedler, H., private communication, 1977.

[32]Hussain, A.K.M.F., "Initial Condition Effect on Free Turbulent Shear Flows," *Structure and Mechanisms of Turbulence I*, edited by H. Fiedler, Springer, New York, 1978, pp. 103-107.